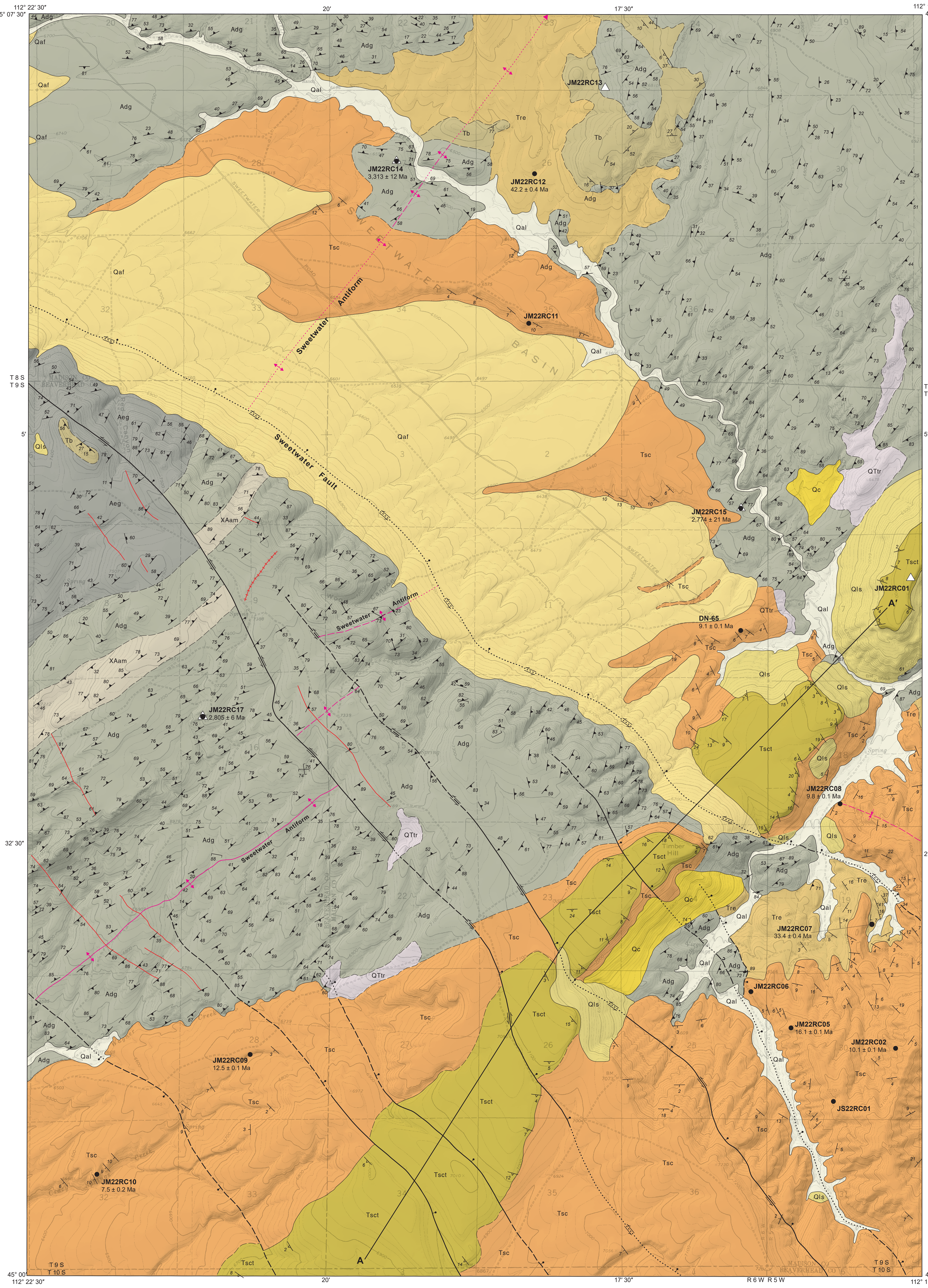

Base map produced by the United States Geological Survey
Red Canyon 1:24,000-scale quadrangle map
Control by: USGS and USC&GC
Compiled from aerial photographs taken 1960
Field checked: 1961
Projection: Polyconic
Vertical Datum: National Geodetic Vertical Datum of 1929
Horizontal Datum: 1927 North American Datum

Shaded relief created from 10-meter digital elevation model from U.S. Geological Survey National Elevation Dataset.

UTM GRID AND 2019 MAGNETIC NORTH DECLINATION AT CENTER OF SHEET
0°56′ 17 MILS
12°6′ 215 MILS

SCALE 1:24,000
CONTOUR INTERVAL 40 FEET
NATIONAL GEODETIC VERTICAL DATUM OF 1929

Maps may be obtained from:
Publications Office
Montana Bureau of Mines and Geology
1300 West Park Street
Butte, Montana 59701-8997
Phone: (406) 496-4174
http://mbmg.mtech.edu

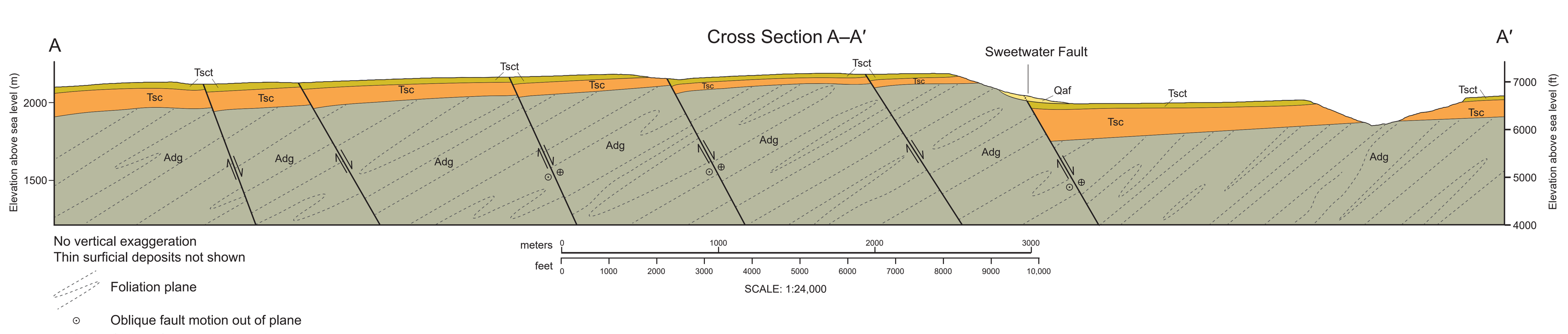

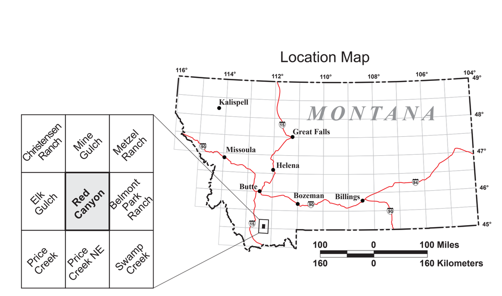

Research supported by the U.S. Geological Survey, National Cooperative Geologic Mapping Program, under USGS award G22AC00376.
GIS production: Jesse Mosolf and Patrica Ekberg, MBMG. Map layout: Susan Smith, MBMG. Editing: Susan Barth, MBMG.

CORRELATION CHART

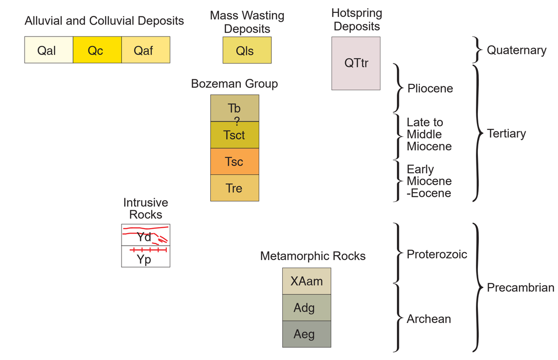

MAP SYMBOLS

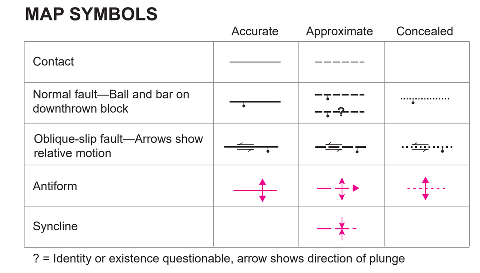

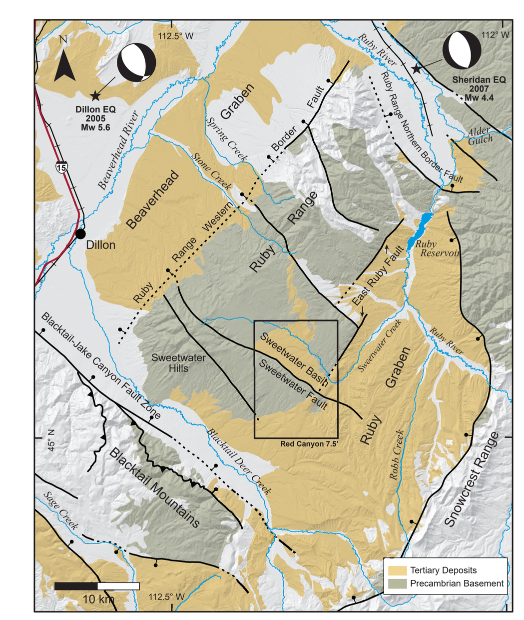

Figure 1. Location and physiographic setting of the map area. Focal mechanisms are shown for recent earthquakes in the region. Simplified geologic map was modified from Ruppel and others (1993) and Vuke and others (2007).

LOCATION AND PHYSIOGRAPHIC SETTING

The Red Canyon 7.5′ quadrangle is in Beaverhead and Madison counties, approximately 32 km (20 mi) southeast of Dillon, Montana. The quadrangle borders the Ruby Graben, covering parts of the Sweetwater Hills and Sweetwater Basin in the southern Ruby Range (fig. 1). The map area is characterized by hilly terrain, grassland, and sparse timber; a prominent escarpment bounding the Sweetwater Hills was likely formed by the Sweetwater fault. Exposure of the bedrock geology and overlying unconsolidated Tertiary–Quaternary deposits is good to excellent. The Red Canyon quadrangle spans a significant drainage divide separating Blacktail Deer and Sweetwater Creeks (fig. 1), both of which are tributaries to the Jefferson River system. The quadrangle elevation ranges from 1,835 to 2,333 m (6,020 to 7,655 ft).

GEOLOGIC SUMMARY

The oldest rock in the map area is Precambrian crystalline basement formed by 3.30–2.77 Ga (Adg and Aeg) and composed primarily of gneiss and layered amphibolite with narrow ribbons of infolded marble, thin layers of pelitic gneiss and schist, and meta-ultramafic rock. The metamorphic assemblages contain several generations of folds, record tectonothermal overprints circa 2.7–1.8 Ga (this study; Okuma, 1971), and are cut by numerous Proterozoic diabase dikes (Yd) and pegmatite intrusions (Yp). The Precambrian basement rocks were deeply exhumed during Late Cretaceous crustal shortening (Carrapa and others, 2019; Mosolf, 2021a), stripping the Paleozoic–Mesozoic sedimentary overburden in the map area.

Poorly consolidated Tertiary sediments composing the Renova and Sixmile Creek Formations of the Bozeman Group nonconformably rest on the Precambrian basement assemblages. The older Renova Formation (Tre) is generally fine-grained and ash-rich, whereas the younger Sixmile Creek Formation (Tsc) comprises coarser sediments interbedded with volcanogenic deposits. The two formations are separated by an angular unconformity that formed during local Miocene extension (Thomas and Sears, 2020). The Timber Hill Basalt member of the Sixmile Creek Formation (Tsct; 6 Ma) forms a prominent mesa in the map area, capping recessive sedimentary members of the Sixmile Creek Formation. The Tertiary and older rocks are displaced by a series of parallel, northwest-striking sinistral normal faults formed during Miocene time (Fritz and Sears, 1993). The Sweetwater fault is the most significant of these structures, with over 200 m (650 ft) of vertical separation and Quaternary movement in the last 130 Ka.

Hot spring deposits with poor age constraints occur locally (QTtr), commonly paralleling bedrock fabrics and faults. Prominent Quaternary alluvial fans (Qaf) onlap the Sweetwater fault escarpment and cover the Bozeman Group and Precambrian rocks in the Sweetwater Basin. Several mass movement deposits (Qls) occur throughout the map area, including a large landslide and rockfall complex rimming the northeast extent of the Timber Hill Basalt member. Extensive alluvial deposits (Qal) have formed along Sweetwater Creek and its tributaries.

PREVIOUS MAPPING

The Red Canyon 7.5′ quadrangle is covered by small-scale mapping by Ruppel and others (1993, scale 1:250,000) and Klepper (1950, scale 1:250,000). Large-scale mapping by Okuma (1971, scale 1:24,000) covered the northwest part of the quadrangle and was focused on the metamorphic basement rocks. Pioneering work on the Precambrian basement rocks in the Ruby Range pertinent to this study was conducted by Garihan (1979a, b), Karasevich (1980), Dahl (1979, 1980), Dahl and Friberg (1980), Desmarais (1981), and James (1990). Ripley (1987, scale 1:24,000) mapped Tertiary sedimentary deposits in the eastern part of the quadrangle; the local Tertiary stratigraphic framework is summarized by Thomas and Sears (2020), Vuke (2020), and references therein.

METHODS

Geologic Mapping

Field mapping was conducted over approximately 3.5 months in 2022 for the STATEMAP component of the United States Geological Survey (USGS) National Cooperative Geologic Mapping Program. A 1:24,000-scale topographic base was utilized for field mapping, and geologic contacts were refined using the orthoimagery dataset produced by the National Agricultural Imagery Program (NAIP; 2018–2020). Structure and observational data were located using a handheld GPS device; structure data were measured with a traditional hand transit or mobile electronic device (Apple iPhone 12). Metamorphic foliations represent all types of recognizable surfaces of metamorphic origin. In gneiss and schist, the foliation commonly parallels mineral compositional layering. Igneous foliations represent surfaces that parallel textures formed by mineral alignment in the groundmass. Field sheets were scanned and georegistered in GIS software. The geologic data were subsequently digitized to the Geologic Map Schema (GeMS) geodatabase mandated by the STATEMAP program.

Whole-Rock Element Chemistry and U-Pb Geochronology

Rock samples collected for whole-rock geochemistry and U-Pb geochronology were processed at the MBMG mineral separation laboratory. A 100- to 200-g split of the crushed material was prepared for bulk-rock geochemical analysis and analyzed by X-ray fluorescence (XRF) and inductively coupled plasma mass spectrometry at the Peter Hooper GeoAnalytical Lab, Washington State University. Zircon was isolated from specimens by standard density and magnetic separation techniques at the MBMG mineral separation laboratory and analyzed by laser ablation inductively coupled plasma mass spectrometry (LA-ICPMS) at the University of California, Santa Barbara.

Whole-rock geochemical data and analytical methods were published by Mosolf and others (2023a). Rare earth element (REE) data from these samples are plotted in figure 2. Table 1 provides U-Pb zircon ages calculated from samples with coherent and interpretable distributions of single-crystal dates; not all samples yielded interpretable emplacement or depositional ages (see Mosolf and others, 2023a). Age distributions obtained for select detrital and metamorphic samples are plotted in figure 3. The complete U-Pb zircon datasets and analytical methods are reported in Mosolf and others (2023b).

DESCRIPTION OF THE MAP UNITS

The Red Canyon geologic map shows rock units exposed at the surface or underlain by a thin surficial cover of soil and colluvium. Surficial sedimentary and mass movement deposits are shown where they are thick and extensive enough to be mapped at 1:24,000 scale. Igneous and metamorphic rocks are classified using the International Union of Geological Sciences nomenclature (Le Bas and Streckeisen, 1991; Schmid and others, 2007). Minerals in igneous and metamorphic units are listed in order of decreasing abundance. Grain size classification of unconsolidated and consolidated sediment is based on the Wentworth scale (Lane, 1947). Multiple lithologies within a rock unit are listed in order of decreasing abundance.

Quaternary Deposits

Extensive alluvial fans (Qaf) onlap the range-front escarpment separating the Sweetwater Hills and Sweetwater Basin. Landslide deposits (Qls) occur throughout the map area and are primarily formed in poorly consolidated Tertiary deposits of the Bozeman Group. Localized hot spring deposits (QTtr) occur along bedrock faults, fractures, or foliation planes (Monroe, 1976; Ripley, 1995). Sweetwater Creek is the only perennial stream in the map area and has formed extensive alluvial deposits in the northern part of the quadrangle.

Qal **Alluvium (Quaternary: Holocene)**—Unconsolidated, poorly to well-sorted, weakly stratified gravel, sand, silt, and clay. Clasts are subangular to rounded cobbles and smaller. Thickness is generally less than 6 m (20 ft).

Qc **Colluvium (Quaternary: Holocene)**—Unconsolidated slope deposit that contains angular, poorly sorted pebbles, cobbles, and boulders. Includes talus. Thickness is generally less than 10 m (33 ft).

Qaf **Alluvial-fan deposit (Quaternary: Holocene and Pleistocene?)**—Unconsolidated, poorly sorted cobbles, gravel, sand, and silt forming extensive, fan-shaped deposits shed from the Sweetwater fault escarpment. Thickness as much as 30 m (100 ft).

Qls **Landslide deposit (Quaternary: Holocene)**—Unstratified, poorly sorted rock fragments deposited by slumps, slides, rock falls, and debris flows. Typically characterized by hummocky topography, subdued landslide scarps, and rock talus. Variable thickness, generally less than 30 m (100 ft).

QTtr **Travertine (Holocene and Tertiary?)**—Deposits of white to gray, massive travertine that generally lacks internal structure but is porous locally. Mainly occurs as isolated bodies but is intercalated with Tertiary sedimentary layers locally. Thickness unknown.

Bozeman Group

The Bozeman Group is mapped as two formations in the quadrangle: the Eocene–Oligocene Renova Formation (Tre) and the Miocene Sixmile Creek Formation (Tsc and Tsct). The Renova Formation comprises shale and siltstone of lacustrine origin. The Sixmile Creek Formation is a complex sequence of coarse volcano-fluvial sedimentary deposits, including the informal Timber Hill Basalt, Big Hole River, Anderson Ranch, and Sweetwater members (Thomas and Sears, 2020 and references therein). The Sweetwater member marks the chronostratigraphic base of the Sixmile Creek Formation and consists mainly of conglomeratic deposits derived from the erosion of local basement uplifts and Eocene volcanogenic deposits. A thick sequence of roundstone conglomerate and interbedded tephra composing the Big Hole River and Anderson Ranch members rest on the Sweetwater member and older map units. The Big Hole River, Anderson Ranch, and Sweetwater members were previously defined by lithostratigraphy that proved challenging to map and were lumped as an undivided unit (Tsc). The Timber Hill Basalt member (Tsct) locally caps the Tertiary sequence in the quadrangle and is the northeastern most remnant of a lava flow that can be traced for approximately 50 km (31 mi) along an ancestral paleovalley extending from Lima to the upper Ruby Valley (Sears, 1995). The basalt forms a prominent mesa in the quadrangle, inverting the topography of the paleovalley it armored. Scattered outcroppings of basalt in the northern part of the quadrangle (Tb) are possibly equivalent to the Timber Hill Basalt member, or a Pliocene basalt northeast of the map area (approximately 4 Ma; Marvin and others, 1974).

The tephra beds of the Anderson Ranch member erupted from silicic calderas that formed as the Yellowstone hotspot tracked northeastward along the eastern Snake River Plain (Shane and Sears, 1995; Thomas and others, 1995; Perkins and Nash, 2002). In the Blacktail Deer Creek area immediately west of the Red Canyon quadrangle, Perkins and Nash (2002) correlated tephra beds in the Anderson Ranch member with the 14 Ma Owyhee–Humboldt, 12.5 Ma Bruneau–Jarbidge, 10 Ma Twin Falls–Picabo, and 6–4 Ma Heise volcanic fields of the Yellowstone hotspot track (Pierce and Morgan, 1990).

Tb **Basalt, undivided (Pliocene?)**—Flaggy, aphanitic basalt containing sparse olivine phenocrysts (<1 percent). Basalt is vesiculated and brecciated locally, containing accidental clasts of metamorphic basement rock. Typically altered and weathers to a rusty red color. Occurs as scattered outcrops in the northern half of the quadrangle. Thickness unknown.

Tsct **Timber Hill Basalt member of the Sixmile Creek Formation (late Miocene)**—Basalt flow that unconformably rests on the recessive Big Hole River member, forming a prominent mesa between Timber Hill and Sweetwater Creek. The interior of the flow is flaggy to massive and mostly aphanitic with <1 percent fresh olivine phenocrysts. Columnar joints are common. Basalt is black to dark gray on a fresh surface and weathers to brown. Reported K-Ar whole-rock ages span 6.3 ± 0.2 Ma to 5.9 ± 0.2 Ma (Fritz and others, 2007). Geochemical data are enriched in light rare earth elements, indicative of fractionation, mixing, or assimilation by parental melts (fig. 2). Thickness is approximately 12 m (40 ft).

Tsc **Sixmile Creek Formation, undivided (late to middle Miocene)**—Weakly consolidated sequence of conglomerate, sandstone, mudstone, and tephra up to 500 m (1,500 ft) thick. Published radiometric age dates for the Sixmile Creek Formation span 16–3.7 Ma, consistent with vertebrate fossil ages (Monroe, 1976; Fritz and Sears, 1993). U-Pb zircon ages obtained in this study span 16.1–7.5 Ma (table 1).

Big Hole River member, informal (Miocene)—Well-sorted, well-rounded fluvial conglomerate that forms crude and possibly channelized bedforms. Conglomerate clasts are typically spherical, pebble to cobble sized, and predominantly composed of quartzite but also include gneiss, basalt, rhyolite, and limestone. Clast lithologies include vitreous pink quartz-arenite, fine-grained white quartz-arenite, black quartz-arenite, black chert laced with quartz veins, and brown cherty litharenite. Subordinate sandstone beds are cross-bedded and form tabular, stepped cliffs. The Big Hole River member rarely crops out and typically forms gravel-draped hillslopes.

Anderson Ranch member, informal (Miocene)—Distinct white, friable beds of tephra up to 30 m (100 ft) thick that are interlayered with roundstone conglomerate, sandstone, and mudstone. Best exposed in low cliffs located in the drainage bottom east of Timber Hill (section 24, T. 9 S., R. 6 W.). The tephra beds are generally lenticular, trough cross-bedded and composed of a mix of ash and pumice, silicic sand and gravel, and tabular to irregular fragments of tuffaceous rip-up clasts. The tephra beds are interfingered with conglomeratic deposits of the Big Hole River member and commonly capped by well-cemented caliche deposits. The Anderson Ranch member is distinguished from tephra-rich members of the Renova Formation by sparse bentonitic clay (Monroe, 1976).

Sweetwater Creek member, informal (earliest middle Miocene)—Interbedded conglomerate and feldspathic sandstone intervals lithologically distinct from the Big Hole River member. Conglomerates are channelized and trough cross-bedded deposits of clast-supported, angular to subangular pebbles and cobbles in a coarse, sandy matrix. Clasts are mainly derived from local Precambrian basement and Eocene volcanic rocks. Brown interbeds of immature, medium to coarse sandstone are up to 1 m (3 ft) thick, massive to cross-bedded, and contain ash, pumice, and small lithic fragments (<4 mm) locally.

Tre **Renova Formation, undivided (Eocene to Oligocene)**—Slope forming sequence of light-colored smectitic fissile shale, siltstone, and limestone with subordinate intervals of sandstone, conglomerate, and tuff that are generally well stratified. Contains fossil fish, insect, leaf, and vertebrate fossils of Arikareean age (Becker, 1961; Dorr and Wheeler, 1964; Monroe, 1976; Ripley, 1987). Typically forms low rounded hills with outcrops limited to gullies and steep bluffs; best exposed in section 19, T. 9 S., R. 5 E., east of Timber Hill. A siltstone sample at this location (JM22RC07) yielded a maximum depositional U-Pb zircon age of 33.4 ± 0.4 Ma and is likely equivalent to the late Oligocene–early Miocene Passamari member of the Renova Formation in the upper Ruby Valley (Monroe, 1976). A poorly exposed sandstone in the northern part of the map area (sample JM22RC12; section 26, T. 8 S., R. 6 W.) tentatively correlated to the Renova Formation yielded a maximum depositional age of 42.2 ± 0.4 Ma. As thick as 60 m (200 ft).

Precambrian Metamorphic and Intrusive Rocks

The Precambrian metamorphic basement rocks in the Ruby Range can be divided into three northeast-trending belts, the Christensen Ranch Metasedimentary Suite, the Dillon Gneiss, and the Elk Gulch Suite; only the latter two units are exposed in the quadrangle where gneiss and amphibolite enriched in incompatible elements are the dominate lithologies observed (fig. 2). The Elk Gulch Suite and Dillon Gneiss are intensely deformed and commonly contain northeast-striking isoclinal folds. Geochronology data suggest that basement protoliths had formed by 3.30–2.77 Ga with tectonothermal overprints of the Beaverhead/Tendoy and Big Sky orogenies occurring at approximately 2.45 Ga and 1.78 Ga, respectively (fig. 3; this study; Harms and Baldwin, 2020; Jones, 2008; Cramer, 2015).

The Elk Gulch Suite is the structurally deepest metamorphic assemblage in the Ruby Range and is inferred to be the oldest. The petrologically diverse assemblage is composed of gneiss, migmatite, and amphibolite. The Dillon Gneiss is a massive to foliated granitic gneiss that is enriched in incompatible elements (fig. 2) and contains abundant intercalations of amphibolite. The Elk Gulch Suite and Dillon Gneiss are difficult to differentiate in the field; the former tends to be more mafic and richer in plagioclase (Garihan, 1979b). Amphibolite occurs throughout both metamorphic assemblages but is only mapped in areas with intercalations thick and abundant enough to be shown at 1:24,000 scale.

Northwest-striking diabase dikes generally crosscut the metamorphic fabric in the crystalline basement rocks and commonly parallel northwest-striking fractures and faults. Wooden and others (1978) described the diabase in the Ruby Range as low potassium tholeiite with a whole-rock Rb-Sr age of 1.4 Ga. A single northeast-striking pegmatite dike of unknown age was identified in the quadrangle; Giletti (1966) reported radiometric ages of approximately 1.6 Ga for pegmatites in the adjacent Christensen Ranch quadrangle, and Mosolf (2021b) reported U-Pb zircon ages of approximately 1.7 Ga from a pegmatite dike swarm intruding the Archean basement near Virginia City.

Yd **Diabase (Mesoproterozoic?)**—Diabase dikes are approximately 1–30 m (3–100 ft) thick with continuous lengths exceeding approximately 1 km (0.6 mi). Diabase is recessive and weathers to spheroidal boulders, commonly creating topographic sags. The rock is frequently altered to secondary minerals, but original diabasic and gabbroic textures are well preserved. Primary minerals appear to have been plagioclase and pyroxene, with minor amounts of quartz, magnetite, and ilmenite. Secondary minerals include chlorite, and sericite. Wooden and others (1978) reported a single Rb-Sr age of approximately 1.4 Ga for the diabase occurring in the area.

Yp **Pegmatite (Mesoproterozoic?)**—A single pegmatite dike (< 2 m; ~6 ft thick) was identified in the west-central part of the map area where it intrudes the Dillon Gneiss. The pegmatite contains brittle fractures but is not foliated and is composed of coarse microcline and quartz with minor amounts of albite-oligoclase. Muscovite from a zoned pegmatite in the adjacent Christensen Ranch quadrangle yielded a K-Ar age of 1.66 Ga and an Rb-Sr age of 1.65 Ga (Giletti, 1966).

XAam **Amphibolite (Archean or Early Proterozoic)**—Black and white, massive- to well-foliated, sheet-like bodies primarily composed of fine- to coarse-grained hornblende, plagioclase, and quartz. Amphibolite typically occurs as two compositional varieties: gneiss containing 40–50 percent hornblende in alternating hornblende-rich and quartz-plagioclase rich layers; or hornblende with accessory plagioclase and quartz. The presence of garnet varies locally from approximately 0 to 25 percent. Amphibolite is intercalated with the other basement assemblages, ranging in size from centimeter-scale lenses to extensive sheets that are tens of meters thick.

Adg **Dillon Gneiss (Archean)**—Gray to reddish-brown, massive to well-foliated, medium- to coarse-grained, locally garnetiferous gneiss of granitic composition that typically forms large, rounded outcrops. Potassium feldspar is the most abundant mineral, intergrown with oligoclase and quartz in nearly equal proportions. Subordinate mineral constituents include biotite, muscovite, garnet, and fibrous sillimanite. Weakly to weakly foliated gneiss often grades into a strongly banded gneiss with a greater abundance of darker minerals, including biotite, garnet, and occasional hornblende. The Dillon Gneiss includes subordinate layers and pods of amphibolite, narrow ribbons of infolded marble, thin layers of pelitic gneisses and schists, and meta-ultramafic rock. Originally named the "Dillon Granite Gneiss" (Heinrich, 1960) and subsequently referred to as "Quartzofeldspathic Gneiss" by James (1990). Stotter (2019) suggested the assemblage be renamed the "Dillon Gneiss," adopted in this map. U-Pb zircon data constrain a minimum emplacement age between approximately 3.3 and 2.7 Ga (fig. 3).

Aeg **Elk Gulch Suite (Archean)**—Diverse assemblage of biotite gneiss, hornblende gneiss, augen gneiss, migmatite, and amphibolite. The most abundant rock type is a banded migmatic gneiss composed of conspicuous dark layers of biotite and hornblende that alternate with layers consisting primarily of quartz and feldspar. Layers of pelitic schists and gneisses are common throughout the unit. Overall, the Elk Gulch Suite is more mafic and aluminous than the Dillon Gneiss. This unit was previously named the "pre-Cherry Creek Group" (Heinrich, 1960) and "Older Gneiss and Schist" (James, 1990). Stotter (2019) renamed the assemblage the Elk Gulch Suite after its type locality, which was adopted in this map.

STRUCTURAL GEOLOGY

Precambrian Deformation

Crystalline rocks of the Dillon Gneiss and Elk Gulch Suite are intensely deformed, with several generations of folds evident in outcrop and map patterns. A penetrative foliation is generally parallel to compositional and migmatic layering (fig. 4), and appears to be penetrative across the Dillon Gneiss and Elk Gulch Suite. Widespread isoclinal folding is mostly axial planar to the main metamorphic foliation and readily visible in outcrops of the Dillon Gneiss assemblage. Most of the isoclinal folds plunge northeasterly, with parallel folds being most common, and similar folds are observed locally. Isoclinal folds are refolded by at least two subsequent generations of folds likely formed during a single orogenic pulse (Okuma, 1971). The primary metamorphic foliation is folded by the map-scale Sweetwater Creek Antiform that plunges 18 degrees to the northeast. Diabase and pegmatite dikes crosscut the older deformational fabrics and folds, constraining early metamorphism and folding prior to 1.7–1.4 Ga. Previously published geochronology ages (e.g., Harms and Baldwin, 2020; Jones, 2008; Cramer, 2015) and U-Pb zircon data from this study (fig. 3) record igneous and tectonothermal pulses circa 2.77 Ga, 2.5–2.4 Ga (Beaverhead/Tendoy orogeny), and 1.8–1.7 Ga (Big Sky orogeny).

Cordilleran Thrust Belt Deformation

Paleozoic–Mesozoic strata that unconformably rest on the crystalline basement in the northern Ruby Range are deformed by Late Cretaceous folds and faults (Tysdal, 1976). In the southern part of the range, the Phanerozoic cover was exhumed and completely eroded during crustal shortening, exposing the Precambrian basement rocks in the Red Canyon quadrangle. Cordilleran structures were not readily identified in the map area, but northwest-striking extensional faults likely overprint and perhaps invert older shortening structures. Additionally, the age of the Sweetwater Creek Antiform is poorly constrained and plausibly formed or was further folded during Late Cretaceous crustal shortening after earlier Precambrian deformation. Low-temperature thermochronology data from the northern part of the Ruby Range suggest rapid cooling, and inferred tectonic exhumation of the basement rocks was underway by approximately 80 Ma (Carrapa and others, 2019).

Cenozoic Extensional Deformation

The Tertiary and older map units are cut by a series of high-angle, northwest-trending extensional faults with a prolonged slip history, extending from the Precambrian to the present (Schmidt and Garihan, 1983). The Sweetwater fault is the most prominent in the map area, forming a steep escarpment bounding the southwest margin of the Sweetwater Basin. The fault has a demonstrable normal component of separation, offsetting the Timberhill Basalt member down-to-the-northeast approximately 200–250 m (655–820 ft; fig. 5; Stickney and Bartholomew, 1987; Ostenaa and Wood, 1990). Tertiary growth strata are preserved in both the hanging wall and footwall blocks of the Sweetwater fault, indicating it was active during periods of late Eocene through Miocene crustal extension and contemporaneous sedimentation. The fault may have a previously undocumented oblique-slip component, sinistrally offsetting the Sweetwater Creek Antiform approximately 2.8 km (1.7 mi); however, it's unclear if the antiformal traces used as piercing points are derived from a single, contiguous structure. Furthermore, the Timber Hill Basalt member has minor lateral offsets, requiring large oblique-slip fault motions before 6 Ma, possibly as an accommodation zone to the East Ruby fault (fig. 1). The southern trace of the East Ruby fault (fig. 1) may project into the Red Canyon quadrangle, where it is obscured by Quaternary deposits and possibly truncated by the northwest-striking Sweetwater fault (Thomas and others, 1995; Sears and others, 2009).

Fault scarps are not readily observed in the field; however, the Sweetwater fault is presumed to be Quaternary-active (e.g., Stickney and Bartholomew, 1987; Ostenaa and Wood, 1990). Using the Timber Hill Basalt member (6 Ma) as a structural datum, the fault's average slip rate is approximately 0.03–0.04 mm/yr (0.001–0.002 in/yr; Stickney and Bartholomew, 1987; Fritz and Sears, 1993).

ACKNOWLEDGMENTS

Connie Thomson, Daniel Brennan, Stuart Parker, and Amanda Rossi performed mineral separations at the MBMG Mineral Separation Laboratory. Andrew Kylander-Clark supported LA-ICPMS analyses and data reduction at the University of California, Santa Barbara. Ashley and Arron Steiner directed bulk-rock geochemical analyses at the Washington State University Peter Hooper Geoanalytical Laboratory. Yann Gavillot and Catherine McDonald provided technical review of the draft map report.

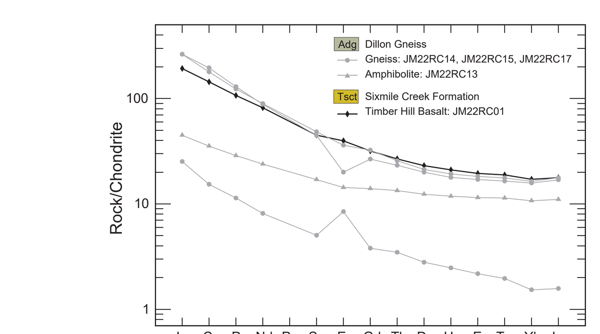

Figure 2. Chondrite-normalized rare earth element diagram of Archean basement rocks and the Timber Hill Basalt member. Plot after Sun and McDonough (1989).

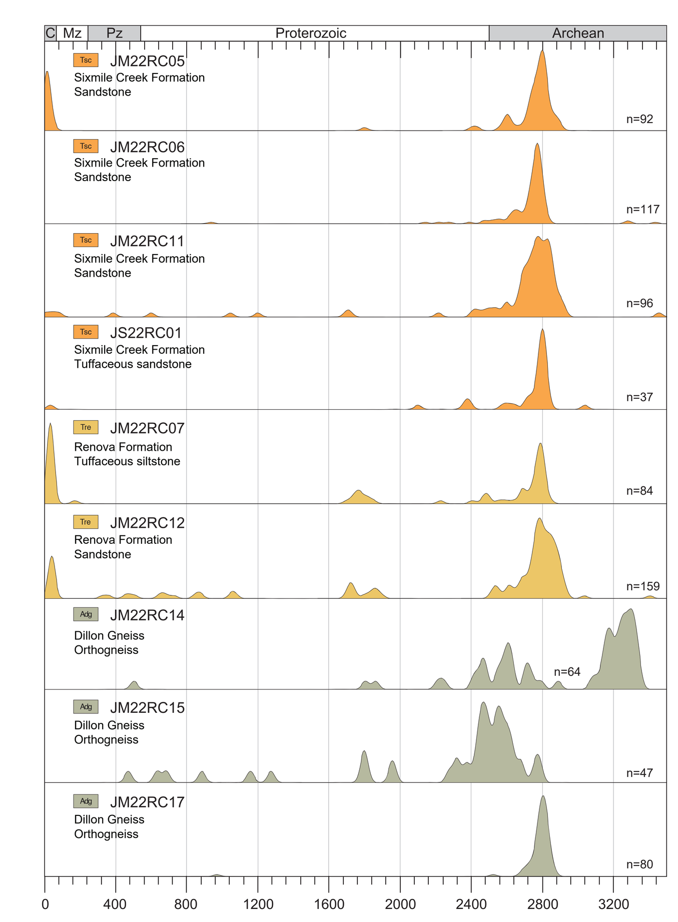

Figure 3. Kernel density estimate (KDE) plots of the ^{207}Pb corrected $^{206}Pb/^{238}U$ (<1,400 Ma) and $^{207}Pb/^{206}Pb$ (>1,400 Ma) zircon age data. KDE bandwidths and bin widths are 20 m.y. A discordance filter was not applied to the data. C, Cenozoic, Mz, Mesozoic, Pz, Paleozoic.

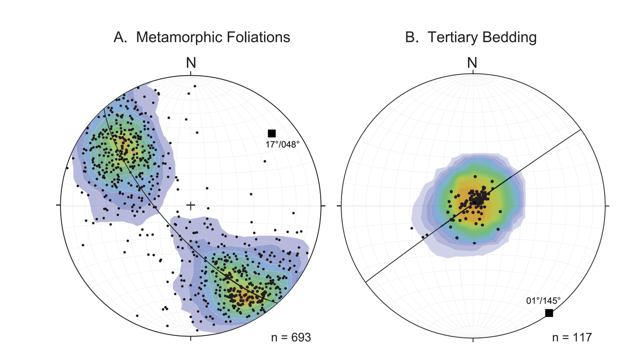

Figure 4. Lower-hemisphere projection of poles to metamorphic foliation (A) and bedding (B) measurements. The data are plotted on an equal-area stereonet and fit with a Kamb contour. The great circle represents the cylindrical best fit of the data, with the corresponding fold hinges marked by a black square labeled with plunge and trend.

REFERENCES

Becker, H.F., 1961, Oligocene plants from the upper Ruby River Basin, southwestern Montana: Geological Society of America Memoir 82, 127 p.
Carrapa, B., DeCelles, P.G., and Romero, M., 2019, Early inception of the Laramide orogeny in southwestern Montana and northern Wyoming: Implications for models of flat-slab subduction: Journal of Geophysical Research: Solid Earth, v. 124, p. 2102–2123.
Cramer, M., 2015, Proterozoic tectonometamorphic evolution of the Ruby Range, SW Montana, USA: Insights from phase equilibria modeling and in situ monazite petrochronology: Missoula, University of Montana, M.S. thesis, 120 p.
Dahl, P.S., 1979, Comparative geothermometry based on major-element and oxygen isotope distributions in Precambrian metamorphic rocks from southwestern Montana: American Mineralogist, v. 64, p. 1280–1293.
Dahl, P.S., 1980, The thermal-compositional dependence of Fe2+-Mg distributions between coexisting garnet and pyroxene-applications to geothermometry: American Mineralogist, v. 65, p. 854–866.
Dahl, P.S., and Friberg, L.M., 1980, The occurrence and chemistry of epidote-clinozoisites in mafic gneisses from the Ruby Range, southwestern Montana: University of Wyoming Contributions to Geology, v. 18, no. 2, p. 77–82.
Desmarais, N.R., 1981, Metamorphosed Precambrian ultramafic rocks in the Ruby Range, Montana: Precambrian Research, v. 16, p. 67–101.
Dorr, J.A. Jr., and Wheeler, W.H., 1964, Cenozoic paleontology, stratigraphy, and reconnaissance geology of the upper Ruby River basin, southwestern Montana: Contributions to Museum of Paleontology, University of Michigan, v. 13, p. 297–339.
Fritz, W.J., and Sears, J.W., 1993, Tectonics of the Yellowstone hotspot wake in southwestern Montana: Geology, v. 21, p. 427–430.
Fritz, W.J., Sears, J.W., McDowell, R.J., and Wampler, J.M., 2007, Cenozoic volcanic rocks of southwestern Montana: Northwest Geology, v. 36, p. 91–110.
Garihan, J.M., 1979a, Geology and structure of the central Ruby Range, Madison County, Montana Summary: Geological Society of America Bulletin, Part I, v. 90, no. 4, p. 323–326.
Garihan, J.M., 1979b, Geology and structure of the central Ruby Range, Madison County, Montana: Geological Society of America Bulletin, Part II, v. 90, p. 695–788.
Giletti, B.J., 1966, Isotopic ages from southwestern Montana: Journal of Geophysical Research, v. 71, p. 4029–4036.
Harms, T.A., and Baldwin, J.A., 2020, Paleoproterozoic geology of Montana, *in* Metesh, J.J., and Vuke, S., eds.: Montana Bureau of Mines and Geology Special Publication 122: Geology of Montana—Geologic History, v. 1, 65 p., available at http://www.mbmg.mtech.edu/pubs/GeologyofMontana/
Heinrich, E.W., 1960, Geology of the Ruby Mountains and nearby areas in southwestern Montana, *in* Pre-Beltian geology of the Cherry Creek and Ruby Mountains areas, southwestern Montana: Montana Bureau of Mines and Geology Memoir, v. 38, p. 31–62.
James, H.L., 1990, Precambrian geology and bedded iron deposits of the southwestern Ruby Range, Montana: U.S. Geological Survey Professional Paper, v. 1495, p. 1–39.
Jones, C.L., 2008, U-Pb geochronology of monazite and zircon in Precambrian metamorphic rocks from the Ruby Range, SW Montana: Deciphering geological events that shaped the NW Wyoming province: Kent, Kent State University, M.S. thesis, 119 p.
Karasevich, L.P., 1980, Structure of the pre-Beltian metamorphic rocks of the northern Ruby Range, southwestern Montana: Harrisburg, Pennsylvania State University, M.S. thesis, 172 p.
Klepper, M.R., 1950, Geologic reconnaissance of parts of Beaverhead and Madison counties, Montana: U.S. Geological Survey Bulletin 969-C, p. 55–85, scale 1:250,000.
Lane, E.W., 1947, Report of the subcommittee on sediment terminology: Transactions of the American Geophysical Union, v. 28, no. 6, p. 936–938.
Le Bas, M.J., and Streckeisen, A.L., 1991, The IUGS systematics of igneous rocks: Journal of the Geological Society of London, v. 148, p. 825–833.
Marvin, R.F., Wier, K.L., Mehnert, H.H., and Merritt, V., 1974, K-Ar ages of selected Tertiary igneous rocks in southwestern Montana: Isochron/West, v. 10, p. 17–20.
Monroe, J.S., 1976, Vertebrate paleontology, stratigraphy, and sedimentation of the upper Ruby River basin, Madison County, Montana: Missoula, University of Montana, Ph.D. dissertation, 301 p.
Mosolf, J.G., 2021a, Geologic map of the Eli Spring 7.5′ quadrangle, Beaverhead County, Montana: Montana Bureau of Mines and Geology Geologic Map 81, 1 sheet, scale 1:24,000.
Mosolf, J.G., 2021b, Geologic map of the Virginia City 7.5′ quadrangle, Madison County, Montana: Montana Bureau of Mines and Geology Geologic Map 80, 1 sheet, scale 1:24,000.
Mosolf, J.G., Brennan, D.T., Gavillot, Y., Parker, S., and Sears, J., 2023a, Major oxide and trace element analyses of rock samples collected in the Dillon and Hamilton 30′ x 60′ quadrangles, southwest Montana: Montana Bureau of Mines and Geology Analytical Dataset 2, https://doi.org/10.59691/WFDT5933
Mosolf, J.G., Brennan, D.T., and Kylander-Clark, A., 2023b, U-Pb geochronology data from rock samples collected in the Dillon, Ennis, Gardiner, Hamilton, Hebgen Lake, Lima, and Wisdom 30′ x 60′ quadrangles, western Montana, 2022–2023: Montana Bureau of Mines and Geology Analytical Dataset 5, https://doi.org/10.59691/ZQRI9918
Okuma, A.F., 1971, Structure of the Southwestern Ruby Range near Dillon, MT: Harrisburg, State College, Pennsylvania State University, Ph.D. dissertation, 122 p.
Ostenaa, D., and Wood, C., 1990, Seismotectonic study for Clark Canyon Dam, Pick-Sloan Missouri Basin Program, Montana: U.S. Bureau of Reclamation Seismotectonic Report 90-4, 78 p., 1 pl.
Perkins, M.E., and Nash, B.P, 2002, Explosive silicic volcanism of the Yellowstone hotspot: The ash fall record: Geological Society of America Bulletin, v. 114, p. 367–381.
Ripley, A., 1987, Paleoenvironmental interpretation of Tertiary carbonates in western Montana: Missoula, University of Montana, M.S. thesis, 99 p.
Ripley, A., 1995, Tertiary carbonates in the upper Ruby and Jefferson River Valleys, Montana: Northwest Geology, v. 25, p. 47–77.
Ruppel, E.T., O'Neill, J.M., and Lopez, D.A., 1993, Geologic map of the Dillon 1º x 2º quadrangle, Idaho and Montana: U.S. Geological Survey Miscellaneous Investigations Series Map I-1803-H, scale 1:250,000.
Schmid, R., Fettes, D., Harte, B., Davis E., and Desmons, J. A., 2007, Systematic nomenclature for metamorphic rocks: 1. How to name a metamorphic rock. Recommendations by the IUGS Subcommission on the Systematics of Metamorphic Rocks, available at https://www.bgs.ac.uk [Accessed March 2023].
Schmidt, C. J., and Garihan, J. M., 1983, Laramide tectonic development of the Rocky Mountain foreland of southwestern Montana, *in* Lowell, J.D. and Gries, R., eds.: Rocky Mountain foreland basins and uplifts: Rocky Mountain Association of Geologists, p. 271–294.
Sears, J.W., 1995, Middle Miocene rift system in SW Montana: Implications for the initial outbreak of the Yellowstone hotspot: Northwest Geology, v. 25, p. 43–46.
Sears, J.W., Hendrix, M.S., Thomas, R.C., and Fritz, W.J., 2009, Stratigraphic record of the Yellowstone hotspot track, Neogene Sixmile Creek Formation grabens, southwest Montana: Journal of Volcanology and Geothermal Research, v. 188, p. 250–259.
Shane, P.A., and Sears, J.W., 1995, Miocene tephra beds in SW Montana: Geochronology, geochemistry and implications: Geological Society of America, Abstracts with Programs, v. 27, no. 4, p. 55.
Stickney, M.C., and Bartholomew, M.J., 1987, Seismicity and late Quaternary faulting of the northern Basin and Range province, Montana and Idaho: Bulletin of the Seismological Society of America, v. 77, p. 1602–1625.
Stotter, S.V., 2019, Determining the Precambrian structure and thermotectonic evolution of the central Ruby Range, southwest Montana: Missoula, University of Montana, M.S. thesis, 78 p.
Sun, S.S., and McDonough, W.F., 1989, Chemical and isotope systematics of oceanic basalts: Implications for mantle composition and processes, *in* Saunders, A.D., and Norry, M.J., eds., Magmatism in the ocean basins: Geological Society, London, Special Publications, v. 42, p. 313–345.
Thomas, R.C., Sears, W.S., Ripley, A.A., and Berg, R.B., 1995, Tertiary extensional history of southwestern Montana: Field trip guide for the Sweetwater and upper Ruby valleys, Montana: Northwest Geology, v. 25, p. 5–25.
Thomas, R.C., and Sears, J.W., 2020, Middle Miocene through Pliocene sedimentation and tectonics in Montana: A record of the outbreak and passage of the Yellowstone Hotspot, *in* Metesh, J.J., and Vuke, S., eds.: Montana Bureau of Mines and Geology Special Publication 122: Geology of Montana—Geologic History, v. 1, 25 p., available at http://www.mbmg.mtech.edu/pubs/GeologyofMontana/
Tysdal, R.G., 1976, Geologic map of the northern part of Ruby Range, Madison County, Montana: U.S. Geological Survey, Miscellaneous Investigations Series Map I-951, scale 1:24,000.
Vuke, S.M., 2020, The Eocene through early Miocene sedimentary record in western Montana, *in* Metesh, J.J., and Vuke, S., eds.: Montana Bureau of Mines and Geology Special Publication 122: Geology of Montana—Geologic History, v. 1, 38 p., available at http://www.mbmg.mtech.edu/pubs/GeologyofMontana/
Vuke, S.M., Porter, K.W., Lonn, J.D., and Lopez, D.A., 2007, Geologic map of Montana: Montana Bureau of Mines and Geology Geologic Map 62, 73 p., 2 sheets, scale 1:500,000.
Wooden, J.L., Vitaliano, C.J., Koehler, S.W., and Ragland, P.C., 1978, The late Precambrian mafic dikes in the southern Tobacco Root Mountains, Montana Geochemistry, Rb-Sr geochronology, and relationship to Belt tectonics: Canadian Journal of Earth Sciences, v. 15, p. 467–479.

TABLE 1. U-Pb zircon geochronology

Sample	Lithology	Unit	Latitude (˚N)	Longitude (˚W)	Method	# of spot analyses[a]	Age (Ma)	2σ	MSWD[b]
JM22RC10	vitric tuff	Tsc	45.0094	112.3662	MDA 206/238	12/50	7.5	0.2	1.4
DN-65	vitric-lithic tuff	Tsc	45.0636	112.2762	WM 206/238	20/40	9.1	0.1	0.9
JM22RC08	pumice tuff	Tsc	45.0467	112.2623	WM 206/238	38/50	9.8	0.1	1.2
JM22RC02	vitric tuff	Tsc	45.0225	112.2545	WM 206/238	38/49	10.1	0.1	2.2
JM22RC09	lithic tuff	Tsc	45.0218	112.3447	MDA 206/238	26/50	12.5	0.1	1.3
JM22RC05	sandstone	Tsc	45.0245	112.2691	MDA 206/238	19/92	16.1	0.1	0.9
JM22RC07	siltstone	Tre	45.0348	112.2579	MDA 206/238	20/84	33.4	0.4	1.3
JM22RC12	sandstone	Tsc	45.1091	112.3051	MDA 206/238	16/159	42.2	0.4	1.3
JM22RC15	gneiss	Adg	45.0759	112.2762	MEA 207/206	3/47	2774.0	21.0	0.6
JM22RC17	gneiss	Adg	45.0552	112.3514	MEA 207/206	69/80	2805.0	5.9	2.1
JM22RC14	gneiss	Adg	45.1103	112.3244	MEA 207/206	13/64	3313.0	12.0	1.5

Note: [a]Numerator is the number of spots used for age calculation; the denominator is the total number of spots analyzed.
[b]MSWD is the Mean Square Weighted Deviation.
Method: WM 206/238 — weighted mean of select $^{206}Pb/^{238}U$ dates
MDA 206/238 — max depositional age, weighted mean of youngest $^{206}Pb/^{238}U$ dates
MEA 207/206 — minimum emplacement age determined by weighted mean of oldest $^{207}Pb/^{206}Pb$ dates
Zircon separates were prepared at MBMG and analyzed by LA-ICPMS at the University of California, Santa Barbara.
Latitudes and longitudes are in the 1984 World Geodetic Survey (WGS84) datum.

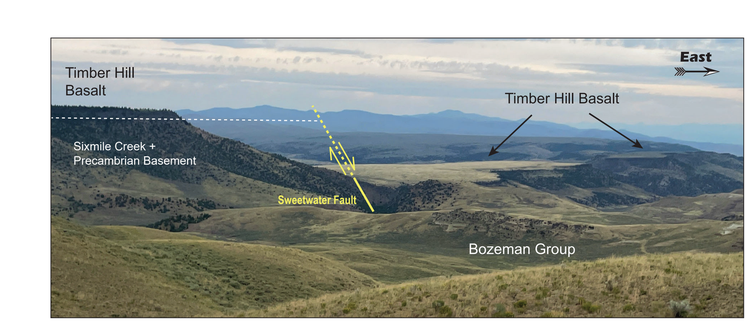

Figure 5. A field photograph looking north shows the northeast extent of the Timber Hill Basalt member (Tsct) resting on Precambrian basement rocks and recessive Tertiary sedimentary deposits of the Bozeman Group. The Sweetwater fault vertically displaces the basalt flow down to the northeast approximately 220 m (660 ft).

MBMG
Montana Bureau of Mines and Geology

Geologic Map 95

Geologic Map of the Red Canyon 7.5′ Quadrangle, Beaverhead and Madison Counties, Montana

Jesse G. Mosolf and James Sears

2024
https://doi.org/10.59691/UJZS2764